

**Gu Figure 1.** (a) Schematic of a backward SHG configuration. (b) Wavelength scan showing phase-matching locations for backward SHG. Arrows indicate theoretically-predicted phase-matching wavelengths.

by using much lower pump energy per pulse.

In conclusion, we have demonstrated, for the first time to our knowledge, BSH generation in periodically-poled bulk  $\text{LiNbO}_3$ , which we believe is a significant first step toward realizing mirrorless OPOs and other unique backward parametric configurations.

## References

1. See *e.g.*, S.E. Harris, "Proposed backward wave oscillation in the infrared," *Appl. Phys. Lett.* **9**, 114 (1966).
2. Y.J. Ding and J.B. Khurgin, "Backward optical parametric oscillators and amplifiers," *IEEE J. Quantum Electron.* **32**, 1574 (1996); Y.J. Ding and J.B. Khurgin, "Second-harmonic generation based on quasi-phase-matching: A novel configuration," *Opt. Lett.* **21**, 1445 (1996).
3. J.A. Armstrong *et al.*, "Interaction between light waves in nonlinear dielectric," *Phys. Rev.* **127**, 1918 (1962).
4. See *e.g.*, E.J. Lim *et al.*, "Blue-light generation by frequency-doubling in periodically-poled lithium niobate channel waveguide," *Electron. Lett.* **25**, 731 (1989).
5. J.U. Kang *et al.*, "Backward second-harmonic generation in periodically-poled bulk  $\text{LiNbO}_3$ ," *Opt. Lett.* **22**, 862 (1997); X. Gu *et al.*, "Backward second-harmonic generation in periodically-poled bulk lithium niobate," *J. Opt. Soc. Am. B* **15**, 1561 (1998).

## Extremely Nonlinear Methyl-red Doped Nematic Liquid Crystal Film

I.C. Khoo, B.D. Guenther, Min-Yi Shih, P. Chen, and W.V. Wood, Electrical Engin. Dept., Penn. State Univ., University Park, PA.

To date, liquid crystals remain an important electro-optics material because of their broadband birefringence. They possess a sizable birefringence,  $\Delta n \sim 0.3$ ,

propagate in opposite directions, the effective interaction length for the process is determined by the pulse duration of the pump. Therefore, for the ultrashort laser pulse, second-harmonic conversion efficiency is reduced significantly.

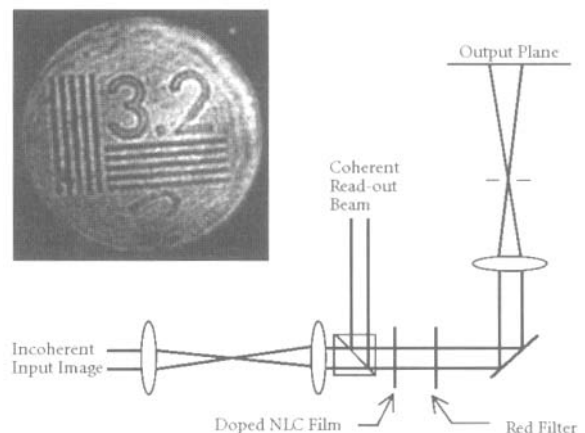
We recently observed BSH generation in a periodically-segmented ion-exchanged potassium titanyl phosphate waveguide. Due to a much shorter period of index gratings, we achieved QPM at much lower orders. Most recently we observed BSH generation in periodically-poled potassium titanyl phosphate waveguide. Because of the presence of the waveguide, we achieved a much higher conversion efficiency

spanning the visible to IR spectral regime.<sup>1</sup> Because of their easy susceptibility to optical fields, they are also well known for their nonlinear optical properties associated with laser induced director axis reorientation effects.<sup>2</sup>

A recent discovery<sup>3</sup> has led to dramatic improvement in both the magnitude of the nonlinear index coefficient and the conditions under which the effect can be generated. A typical nematic liquid crystal, Pentyl Cyano Biphenyl [5CB] with traces of the laser dye methyl-red dissolved in it at a concentration of about 0.5% was used and it was shown that these films are extremely photosensitive and easily yield photocharges and photovoltaic effects from the photo-excited dye dopant. These photo induced DC space charge fields cause the highly birefringent liquid crystalline axis to reorient, giving rise to a large refractive index change for extraordinarily polarized light. In general, the response time of the nematic liquid crystal director axis reorientation is on the order of milliseconds.<sup>1</sup>

In a grating diffraction experiment, a nonlinear index change coefficient  $n_2 = 6 \text{ cm}^2/\text{W}$  was observed.<sup>3</sup> Similar values of  $n_2$  are obtained at other Argon laser lines within the absorption band of the Methyl-red dye. Recent studies show that the effect can be enhanced by an AC field, with an effective  $n_2 > 10 \text{ cm}^2/\text{W}$ , equivalent to a nonlinear third-order susceptibility  $\chi^{(3)} > 300 \text{ esu}$ . This is perhaps the most nonlinear optical material known to date.

Such extremely nonlinear film allows the observation of various nonlinear optical processes at unprecedented low optical power. In particular, self-defocusing and optical limiting of cw laser at nanowatt threshold was demonstrated,<sup>4</sup> as was incoherent-coherent image conversion at  $\mu\text{W}/\text{cm}^2$  light intensity level. Figure 1 depicts the setup used to demonstrate incoherent-coherent image conversion. A slight modification of the setup could also be used for visible to IR [or other wavelength] image conversion applications. The polarized green image bearing beam creates a spatially distributed phase shift on the NLC film, which is read by a coherent (red) He-Ne laser. Visible images can be generated with an input incoherent light intensity as low as  $90 \mu\text{W}/\text{cm}^2$ . This is comparable to the in-



**Khoo Figure 1.** Experimental setup for incoherent to coherent image conversion. Inset is a photograph of the coherent image at He-Ne laser wavelength.

tensity level required for the operation of existing commercial liquid crystal spatial light modulators (SLMs).<sup>5</sup>

One advantage of dye doped nematic liquid crystals over SLMs<sup>5</sup> is the resolution capability. As demonstrated in the study of diffraction efficiency dependence on grating spacing,<sup>3</sup> the resolution can be over 200 lp/mm, compared to commercial SLMs typical resolution capability of at most 40 lp/mm.

### Acknowledgments

This work is supported by the Army Research Office and the Air Force Research Laboratory.

### References

1. I.C. Khoo, *Liquid Crystals: Physical Properties and Nonlinear Optical Phenomena* (Wiley Interscience, New York, NY, 1995). See also, I.C. Khoo and S.T. Wu, *Optics and Nonlinear Optics of Liquid Crystals* (World Scientific Publishing, Riveredge, NJ, 1993).
2. E.V. Rudenko and A.V. Sukhov, "Optically induced spatial charge separation in a nematic and the resultant orientational nonlinearity," *JETP* **78** (6), 875-882, 1994. I.C. Khoo, "Orientational photorefractive effects in nematic liquid crystal film," *IEEE J. Quant. Elect.* **32**, 525-534 (1996), and earlier references therein.
3. I.C. Khoo *et al.*, "Optically induced space-charge fields, dc voltage, and extraordinarily large nonlinearity in dye-doped nematic liquid crystals," *Opt. Lett.* **23**, 253-255 (1998).
4. I.C. Khoo *et al.*, "Nonlinear optical liquid cored fiber array and liquid crystal film for ps-cw frequency agile laser optical limiting application," *Op. Ex.* **2** (12), (1998).
5. M.T. Gruneisen and J.M. Wilkes, "Spatial light modulators," G. Burdge and S.C. Esener, eds., *OSA TOPS* **14**; see also M.A. Kramer *et al.*, "One-way imaging through an aberrator with spatially incoherent light using an optically addressed spatial modulator," *Appl. Opt.* **30**, 3319-3323 (1991).

## OPTICAL ENGINEERING

### Photonic Time-stretch Offers Solution to Ultrafast Analog-to-digital Conversion

B. Jalali, F. Coppinger, and A.S. Bhushan, Univ. of California at Los Angeles, Los Angeles, CA.

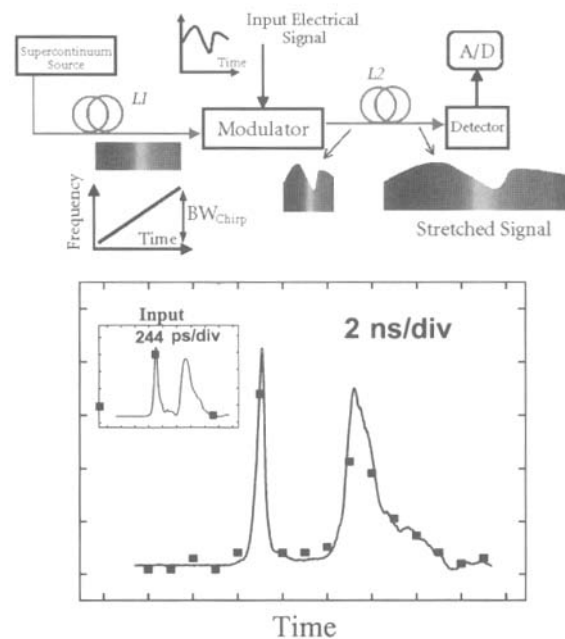
**A**nalog-to-digital (A/D) conversion represents the key bottleneck in high performance radar and communication systems. The current trend in electronic receivers is to perform the conversion at microwave frequencies. In the so-called "digital receiver," the A/D conversion is performed at microwave (carrier) frequencies, thus placing stringent requirements on the sampling frequency and input bandwidth of the A/D. It is widely recognized that new concepts leading to major advances in A/D technology are a priority.

Recently, a new optically-assisted A/D concept was proposed and demonstrated.<sup>1</sup> The electrical signal is time-stretched in the optical domain, prior to sampling and quantization. By reducing the signal bandwidth, the new concept offers revolutionary enhancements in input bandwidth and sampling rate of A/D converters. Further, the noise due to sampling jitter is reduced. Performing the time-stretch in the optical domain is critical as it ensures that both the microwave carrier and its modulation are slowed down.<sup>2</sup> This scheme can be applied to both finite-

time as well as continuous-time waveforms. In the latter case, the signal is first segmented and interleaved into  $m$  channels and each segment is stretched by a factor  $m$ .<sup>1</sup>

While the basic concept of time-stretching has been known for nearly 30 years,<sup>3,4</sup> its practical implementation has not been successful due to the difficulty of obtaining high chirp rates or highly dispersive elements. In the demonstration of the time-stretch analog-to-digital converter (TS-ADC) shown in Figure 1, pulses from a modelocked erbium-doped fiber ring laser are compressed in a nonlinear fiber to obtain a 7.5-THz supercontinuum, which is subsequently chirped in a single-mode fiber of length  $L_1$ . The intensity of this chirped pulse is modulated with the input electrical signal, hence mapping time into optical wavelength. The intensity-modulated chirped pulse is then dispersed in a fiber of length  $L_2$ , stretching the modulation envelope. Since the bandwidth of the optical pulse (1-20 THz) is much larger than the electrical bandwidth (< 100 GHz), dispersion-induced signal distortion is negligible.<sup>2</sup> The entire function is implemented with optical fibers and guided wave devices resulting in a compact and rugged system. The stretch factor is approximately given by  $M \sim (L_1 + L_2)/L_1 = 8$ .<sup>2</sup> The stretched envelope is detected and digitized with an electronic A/D converter with a sample rate of 1 Gs/s and input bandwidth of 500 MHz.

The solid line in Figure 1b shows the waveform captured by the sampling oscilloscope. The data points, spaced 1 ns apart, represent digitized output of the ADC. The inset shows the waveform prior to time stretching. Clearly, the electronic ADC with 1 ns sample interval is unable to capture the waveform. However, after time-stretching, bandwidth of the analog waveform is reduced by the stretched factor,  $M = 8$ , allowing it to be captured



**Jalali Figure 1.** Simple time-stretch system (top) and preliminary demonstration of time-stretch A/D conversion (bottom). Data points are the digitized samples and the solid line is the analog waveform. The inset shows the output without time-stretch.